

University of Wollongong

Research Online

Faculty of Science, Medicine and Health -
Papers: part A

Faculty of Science, Medicine and Health

1-1-2012

A deep subaqueous fan depositional model for the Paleoarchaean (3.46 Ga) Marble Bar Cherts, Warrawoona Group, Western Australia

Nicolas Olivier
Universite de Lyon

Gilles Dromart
Universite de Lyon

Nicolas Coltice
Institut Universitaire de France

Nicolas Flament
Universite de Lyon, nflament@uow.edu.au

Patrice F. Rey
University of Sydney

See next page for additional authors

Follow this and additional works at: <https://ro.uow.edu.au/smhpapers>



Part of the [Medicine and Health Sciences Commons](#), and the [Social and Behavioral Sciences Commons](#)

Recommended Citation

Olivier, Nicolas; Dromart, Gilles; Coltice, Nicolas; Flament, Nicolas; Rey, Patrice F.; and Sauvestre, Remi, "A deep subaqueous fan depositional model for the Paleoarchaean (3.46 Ga) Marble Bar Cherts, Warrawoona Group, Western Australia" (2012). *Faculty of Science, Medicine and Health - Papers: part A*. 4385.

<https://ro.uow.edu.au/smhpapers/4385>

Research Online is the open access institutional repository for the University of Wollongong. For further information contact the UOW Library: research-pubs@uow.edu.au

A deep subaqueous fan depositional model for the Paleoarchaeon (3.46 Ga) Marble Bar Cherts, Warrawoona Group, Western Australia

Abstract

The 3.46 Ga Marble Bar Chert Member of the East Pilbara Craton, Western Australia, is one of the earliest and best-preserved sedimentary successions on Earth. Here, we interpret the finely laminated thin-bedded cherts, mixed conglomeratic beds, chert breccia beds and chert folded beds of the Marble Bar Chert Member as the product of low-density turbidity currents, high-density turbidity currents, mass transport complexes and slumps, respectively. Integrated into a channel-levee depositional model, the Marble Bar Chert Member constitutes the oldest documented deep-sea fan on Earth, with thin-bedded cherts, breccia beds and slumps composing the outer levee facies tracts, and scours and conglomeratic beds representing the channel systems.

Disciplines

Medicine and Health Sciences | Social and Behavioral Sciences

Publication Details

Olivier, N., Dromart, G., Coltice, N., Flament, N., Rey, P. & Sauvestre, R. (2012). A deep subaqueous fan depositional model for the Paleoarchaeon (3.46 Ga) Marble Bar Cherts, Warrawoona Group, Western Australia. *Geological Magazine*, 149 (4), 743-749.

Authors

Nicolas Olivier, Gilles Dromart, Nicolas Coltice, Nicolas Flament, Patrice F. Rey, and Remi Sauvestre

1 A deep subaqueous fan depositional model for the Paleoarchean (3.46

2 Ga) Marble Bar Cherts, Warrawoona Group, Western Australia

3
4 NICOLAS OLIVIER†*, GILLES DROMART†*‡, NICOLAS COLTICE†*, NICOLAS
5 FLAMENT†*§, PATRICE REY§, and RÉMI SAUVESTRE¶

6
7 †*Université de Lyon, Lyon, France*

8 **CNRS UMR 5276 Laboratoire de géologie de Lyon, Université Lyon 1, Villeurbanne,*
9 *France*

10 ‡*ChemCam team, Mars Science Laboratory project*

11 §*Earthbyte Group, School of Geosciences, The University of Sydney, NSW 2006, Australia*

12 ¶*Ecole Normale Supérieure de Lyon, Lyon, France*

13
14 †Author for correspondence: Nicolas.Olivier@univ-lyon1.fr

15
16 **Abstract**

17 The 3.46 billion-year-old (Ga) Marble Bar Chert Member of the East Pilbara Craton,
18 Western Australia, is one of the earliest and best-preserved sedimentary successions on Earth.
19 Here, we interpret the finely laminated thin-bedded cherts, mixed conglomeratic beds, chert
20 breccia beds and chert folded beds of the Marble Chert Member as the product of low-density
21 turbidity currents, high-density turbidity currents, mass transport complexes and slumps,
22 respectively. Integrated into a channel-levee depositional model, the Marble Bar Chert
23 Member constitutes the oldest documented deep-sea fan on Earth, with thin-bedded cherts,
24 breccia beds, and slumps composing the outer levee facies tracts, and scours and
25 conglomeratic beds representing the channel systems.

26
27 **Keywords:** Archean, Chert, Deep sea fan, Marble Bar.

30 **1. Introduction**

31 Sedimentary deposits of the Palaeoarchean greenstones of the East Pilbara Craton,
32 Western Australia, are of particular geological significance for hosting the oldest putative
33 microfossils (Schopf, 1993; Schopf *et al.* 2002), the oldest stromatolites (Allwood *et al.* 2006;
34 Van Kranendonk, 2006) and preserving evidence of the environmental conditions of the Early
35 Earth (Robert & Chaussidon, 2006; Hoashi *et al.* 2009; van den Boorn *et al.* 2010). Among
36 these rocks, the c. 3460 Ma Marble Bar Chert Member of the Duffer Formation (Warrawoona
37 Group) is a typical Archean red-white-grey banded chert remarkably exposed at the Marble
38 Bar Pool and Chinaman Pool localities (Fig. 1; Buick & Barns, 1984; Van Kranendonk,
39 2006). Previous studies on the sedimentary rocks of the Marble Bar Chert Member focused
40 on the chemical and thermal conditions associated with the precipitation of these cherts
41 (Sugitani, 1992; Minami *et al.* 1995; Kojima *et al.* 1998; Orberger *et al.* 2006; van den Boorn
42 *et al.* 2007, 2010). However, the depositional environment and the mode of formation of the
43 Marble Bar Cherts remain subject to debate, and both quiet hydrothermal environments on a
44 mid-oceanic ridge and large submarine caldera settings have been proposed (Oliver &
45 Cawood, 2001; Kato & Nakamura, 2003; Van Kranendonk, 2006; Hoashi *et al.* 2009; van den
46 Boorn *et al.* 2010). Hoashi *et al.* (2009) argued that the haematite grains in the Marble Bar
47 Cherts precipitated directly when hydrothermal fluids of temperature greater than 60 °C and
48 rich in reduced iron mixed rapidly with seawater containing oxygen in a submarine volcanic
49 depression at depths between 200 m and 1,000 m. Supporting evidence for such a deep
50 environment for the Marble Bar Chert Member is at best indirect, based on the absence of
51 sedimentological or volcanic features characteristic of shallow water settings (Hoashi *et al.*
52 2009). The presence of oxygen in deep water strongly questions the common view of
53 widespread anoxia throughout the Archean, making essential the scrutiny of the depositional
54 setting of the Marble Bar Chert Member (Konhauser, 2009). This contribution provides a

55 comprehensive description of the sedimentary facies and structures of the Marble Bar Chert
56 Member, along with a depositional model to identify the environmental setting of those
57 ancient rocks. We conclude that the sedimentary rocks of the Marble Bar Chert Member were
58 deposited in a deep sea fan at the toe of an emerged continental mass and that most of these
59 ancient sediments were subjected to short- to long-distance transport.

60

61 **2. Geological setting**

62 The Pilbara Block (Western Australia) consists of a granite-gneiss complex and
63 surrounding greenstone belt (Hickman, 1983). The 3.53-3.165 Ga East Pilbara Terrane – i.e.
64 the ancient nucleus of the Pilbara Craton – is composed of the Pilbara Supergroup, which
65 consists of four volcano-sedimentary groups (Van Kranendonk *et al.* 2007). The lower part of
66 the Pilbara Supergroup is represented by the 3.515-3.427 Ga Warrawoona Group, which
67 recorded prehnite-pumpellyite to greenschist facies metamorphism (Hickman, 1983; Van
68 Kranendonk *et al.* 2007). This Group consists of ultramafic, tholeiitic, felsic lavas and
69 volcanoclastic rocks with subordinate cherts. The Marble Bar Chert Member occurs at the top
70 of the 3.472-3.465 Ga Duffer Formation and is overlaid by the Apex Basalt Formation (Van
71 Kranendonk, 2006). This Member is best exposed at the Marble Bar Pool and Chinaman Pool
72 localities (Fig. 1), 0.5 km away one from another, about 3 km west of Marble Bar.

73 The Marble Bar Chert Member is a well-preserved unit of centimetre-layered red,
74 white and dark blue chert up to 200 m thick (Hickman, 1983; Van Kranendonk *et al.* 2002).
75 This Member displays important thickness variations that repeat at regular intervals over the
76 30 km long band along which it outcrops (Hoashi *et al.* 2009). At the Chinaman Pool and
77 Marble Bar Pool localities, the deposits of the Marble Bar Chert Member – preserved between
78 units of pillow basalt and dipping 70°E – are interpreted to be overturned (Van Kranendonk,
79 2006). The Marble Bar Chert Member displays a well-marked stratigraphic zoning with

80 predominant white and dark-blue chert in the lower part of the unit whereas its uppermost
81 third of the unit displays more dominant red cherts (Kato & Nakamura, 2003; Van
82 Kranendonk *et al.* 2006; Hoashi *et al.* 2009).

83

84 **3. Chinaman Pool and Marble Bar Pool chert facies**

85 A spectacular colour banding is exposed throughout the c. 50 m thick lower Marble
86 Bar pool section, with the alternation of red, white and dark blue cherts (Kato & Nakamura,
87 2003; Van Kranendonk, 2006). Red and dark blue coloured bands are largely dominant over
88 milky white horizons. These contrasted colourations are due to differing amount of minute
89 haematite inclusions in the microquartz matrix of the chert (Buick & Barns, 1984), with some
90 subtle grain size variation of the microquartz visible microscopically (Oliver & Cawood,
91 2001). Red bands are dusted throughout by tiny specs of haematite, goethite, opaque minerals
92 and rhombic carbonate and possible altered bands of pyrite and magnetite (Sugitani, 1992).
93 Haematite-rich microbands of the uppermost section – i.e. Zones IV and V of in Archean
94 Biosphere Drilling Project (ABDP) site 1 (Hoashi *et al.* 2009) – are parallel to the bedding
95 plane and vary from ~0.01 mm to ~1 mm in thickness and <1 cm to >10 m in lateral extent.
96 The microbands are composed of discrete particles (0.1-0.6 μm in diameter) and clusters
97 (0.001-0.1 mm in diameter) of haematite. Dark-blue bands, which are common in the lower
98 section, contain microscopic carbonaceous material (kerogen; Sugitani, 1992). The siderite-
99 rich, lowermost zone described by Hoashi *et al.* (2009) in ABDP site 1 is not exposed at the
100 surface. The most complete section of the Marble Bar Chert Member is located at Chinaman
101 Pool. It is composed of two very distinctive sub-units: 1) a well-bedded, evenly and finely flat
102 laminated lower section characterized by a conspicuous red-white-dark blue banded facies,
103 and prominent brecciated beds locally referred to as “stick beds” (Hickman & Lipple, 1978;
104 Hickman, 1983); and 2) an upper section composed of interbedded chert layers and clastic

105 deposits made of coarse felsic grains (Fig. 1b). At Marble Bar Pool, there is a unique chert
106 unit preserved between two pillow basalt units. It is not clear whether the Marble Bar Chert
107 Member of Chinaman Pool and Marble Bar Pool are part of the same chronostratigraphic unit.
108 Nevertheless, the comparison of lithologies, fabrics and facies at both sites points to
109 comparable depositional environments.

110 The thin-bedded chert facies consist of 0.05-0.40 m thick, evenly and finely laminated
111 beds of black or red cherts (Fig. 2a, b). Lamination is only observed in red and dark-blue
112 cherts and is defined by millimetre-scale variations in granularity and colour (Sugitani, 1992;
113 Van Kranendonk, 2006). Beds of red and dark-blue cherts laterally pinch out as tapered flow
114 margins and sometimes overlie clast-supported layers. Sub-planar, undulose, parallel
115 laminations of red and black cherts are characteristic of tracted and suspended-load flows of
116 low-density currents. The thin-bedded chert facies is interpreted as fine-grained turbidites
117 (e.g. Piper & Stow, 1991). They make up most of the lower Marble Bar Chert Member and
118 are only sporadically present in the upper Marble Bar Chert Member.

119 The beds of the lower Marble Bar Chert Member, up to a few metres thick, contain
120 bed-confined asymmetric folds, disharmonic folds and typical slump boudins (Fig. 2c). Folds
121 are not recumbent and trains have not been observed. Locally, beds either pinch out laterally
122 over a distance of a few meters or display thickening due to minor thrust duplexes (Fig. 2d).
123 All of these features are indicative of post-depositional, layer-confined deformation of semi-
124 consolidated sediments related to cohesive, gravity-driven mass-transports. Slumped beds are
125 restricted to the lower Marble Bar Chert Member.

126 There are two modes of formation for chert breccia material in the lower Marble Bar
127 Chert Member: 1) late breccia bands and hydrothermal fault arrays at high angles to the
128 bedding (Oliver & Cawood, 2001); 2) breccia beds conformable or at low angle to bedded
129 chert and referred to as “stick beds”. The “stick beds” of the Marble Bar Chert Member are

130 typically 0.1-0.5 m thick (Fig. 2e–g). Some beds display marked changes in thickness,
131 pinching and swelling at irregular intervals. Bed thickness commonly doubles at swells. The
132 “stick beds” are completely layer-confined (Fig. 2e). They commonly exhibit sharp and
133 conformable basal boundaries with local compaction of underlying lithologies by clasts (Fig.
134 3a). The “sticks” are angular, sharp-edged, elongated and platy clasts ($L/H > 10$) of milky
135 white chert. They are monogenic, of a lithology similar to the underlying ribbon chert. Clasts
136 are typically arranged in spectacular shingle-like imbrications (long axis sub-parallel to the
137 bedding or inclined 15-35°) and locally in angular folds (Fig. 2e). Some of the “stick beds”
138 show normal grading (Fig. 2f). The “stick beds” are intra-formational breccias, resulting from
139 the fragmentation of shallow buried, early-lithified beds with limited displacement of clasts.
140 In addition to slump folds and boudins, the textural gradation from slumps to breccia beds
141 suggests that the breccia beds are dismembered slumps. The fabric of the “stick beds” is
142 strikingly similar to that of carbonate breccia beds of deep-water slope environments in
143 Phanerozoic sequences (Dromart *et al.* 1993; Robin *et al.* 2010). The “stick beds” are mainly
144 observed in the uppermost section of the lower Marble Bar Chert Member. Other types of
145 breccia beds have been recognized in the Marble Bar Chert Member. They consist of layers of
146 variably elongated ($1 \leq L/H < 10$) pebble- to granule-sized intra-formational white-chert
147 clasts locally displaying normal grading, and locally capped by thin-bedded cherts (i.e. finely
148 laminated beds of red and dark-blue cherts). These observations suggest that depositional
149 processes for chert breccia beds, including “stick beds”, vary from: 1) slumps to, 2)
150 unchannelized mass transport complexes (i.e. cohesive debris flows with only minor evidence
151 of erosion and sporadic evidence of organization as clast imbrications) and to, 3) high-density
152 turbidity currents (i.e. non-graded to graded, clast-supported layers overlain by laminated,
153 turbulent flow fabrics).

154 The upper section of the Marble Bar Chert Member at Chinaman Pool consists of
155 coarse-grained siliciclastic sequences with recurrent thin-bedded cherts (Fig. 2g, h). “Sticks”
156 of typical milky-white chert are observed as floating clasts in a coarse-grained siliciclastic
157 matrix (Fig. 2i). Other lithoclasts of these mixed conglomeratic beds consist of mixed
158 granule- to pebble-sized rounded fragments of mafic (basalt) and felsic (granodiorite) rocks.
159 Sedimentary structures include meter-scale moderately incised channels and some trough-
160 cross beds (Figs 2n, 3b). Inverse to normal grading, multilayering, clast imbrication and
161 outsized clasts are common features (Fig. 2j). We interpret these deposits, except the thin-
162 bedded cherts, to be typical high-density turbidites.

163 An unambiguous meter-scale syn-depositional growth fault is located in the upper
164 section of Chinaman Pool. It consists of a normal, listric fault sealed upwards by chert beds
165 and passing downwards to a subhorizontal shear zone (Fig. 2k, l). The hanging wall block is
166 affected by a typical rollover anticline and supports a sand-filled channel created by the listric
167 fault collapse. This syn-depositional feature makes it an unmistakable stratigraphic polarity
168 criterion. In addition, it suggests that the unconformable surface that bounds the lower and
169 upper Marble Bar Chert Member and shows truncation and onlap stratal termination features
170 (Fig. 2m) was generated by the collapse of a much larger listric fault.

171

172 **4. A channel-levee depositional model for the Marble Bar Chert Member**

173 The set of facies and sedimentary structures, including unconformable surfaces,
174 observed in the Marble Bar Chert Member describes a general channel-levee depositional
175 system (Fig. 2), such as originally described by Mutti (1977). In these gravity-driven
176 depositional systems, the levees of the subaqueous channel-levee systems form from the
177 overbanking of predominantly fine-grained sediment (silts and clays) because of the spill over
178 of turbulent flows as they move down the channel system (Mutti & Normark, 1987; Piper &

179 Deptuck, 1997). Colour-banded mud and clay are the most common sedimentary facies within
180 the overbank deposits, with rare interbeds of coarser sediment composed of silt-size particles
181 occurring in laminae and sharp-based thin beds (Normark & Damuth, 1997). Conversely,
182 channel deposits consist of thick-bedded coarse facies including structureless to chaotic sand
183 beds, graded and cross-bedded sand beds (normal grain-size grading is predominant and many
184 graded sand beds grade upward through silt to clay at top), plus chaotic mud (mud clasts
185 deriving from localized sediment failure from inner levees). The channel deposits of the
186 Marble Bar Chert Member are dominated by coarse-grained siliciclastics. The internal
187 geometry of the channel-fill deposits indicates that the channels were cut prior to and during
188 their infilling. The bedding surfaces of the upper and lower channel deposits tend to be
189 parallel to the flat channel tops and to the irregular channel floors, respectively. Bedding
190 surfaces of lower channel deposits gradually onlap the basal channel surface. Slumping, other
191 mass-flows and late fracture-related deformation have removed the original dip of the levee
192 beds. The bedded cherts of the Marble Bar Chert Member appear to have been indurated
193 before burial compaction, probably very early, at time of sea-floor exposure. The best
194 supportive evidence for early lithification of these cherts comes from the occurrence of cherts
195 as reworked clasts in the mixed conglomeratic facies (Fig. 2j) and from load cast features due
196 to differential compaction of distinctively indurated material (Fig. 3a). Due to early
197 lithification, siliceous levee slopes may display higher angle of repose than typical modern
198 siliciclastic subaqueous levees do (5° at best; e.g. Gervais *et al.* 2001; Mingeon *et al.* 2001;
199 Broucke *et al.* 2004). Slope over-steepening by early lithification combined to slope
200 overloading by high sediment flux on the channel levee would explain the frequent
201 occurrence of slumping and other mass gravity flows observed in the lower Marble Bar Chert
202 Member sequence. Hence, the slumped beds, mass-flow deposits, turbidite beds, and growth

203 faults make a comprehensive assortment of gravity driven sedimentary processes in a slope
204 environment.

205

206 **5. Discussion and conclusion**

207 In the Marble Bar Chert Member, polymictic conglomeratic and pebbly-sandstone
208 units – including granodiorite and basaltic sources –characterize the channel deposits of the
209 channel-levee depositional model-(Fig. 2). This suggests that these 3.456 Ga sediments-were
210 deposited at the toe of emerged and differentiated continental lands, which is consistent with
211 the oldest angular unconformity reported in the East Pilbara Craton (Buick *et al.*, 1995). Thus,
212 the deposits of the Marble Bar Chert Member were not related to a mantle plume as suggested
213 by Kato & Nakamura (2003), nor to mid-ridges and active spreading centres, as proposed by
214 Lascelles (2007). In the northern part of the Marble Bar greenstone belt (Fig. 1), the youngest
215 3.458-3.427 Ga Panorama Formation consists of mudstones and sandstones also interpreted to
216 represent turbidites near a continental margin of a differentiated and evolved continent (Kato
217 & Nakamura, 2003). The only known deep gravity-driven deposits on Earth older than that of
218 the Marble Bar Chert Member are 3700 to 3800 Ma normally graded sandstone layers
219 interpreted as turbidites from the Isua greenstone belt (Rosing, 1999). These sedimentary
220 rocks have been strongly metamorphosed to at least amphibolite facies conditions and are
221 strongly deformed (Nutman, 2006). Thus, complete turbiditic sequences at Isua remain rare
222 and could result from depositional mechanisms other than turbidity flows (Fedo, Myers &
223 Appel, 2001). These putative Isua turbidites are devoid of terrigenous clastic sediments,
224 implying deposition in an oceanic environment in the vicinity of volcanic edifices (Rosing,
225 1999). Because the Marble Bar Chert Member yields a low-grade metamorphism (Van
226 Kranendonk *et al.* 2007), it preserves a unique set of facies documenting the earliest deep-sea
227 fan on Earth.

228 Modern channel-levee complexes are observed in the middle section of deep-water
229 fans downstream of the continental slope break, at very variable water depth (500 – 3000 m;
230 Richards, Bowman & Reading, 1998). Additional sedimentary structures – e.g. wave-driven
231 deposits such as hummocky and swaley cross-beds – that would further constrain the water
232 depth were not observed. Thus, a depth range of 200 to 1000 m proposed for the depositional
233 setting of the Marble Bar Chert Member (Hoashi *et al.* 2009) appears to be minimal.

234 The red cherts of the Marble Bar Chert Member are made of silt-sized clusters of
235 haematite crystals (Sugitani, 1992; Hoashi *et al.* 2009). Hoashi *et al.* (2009) argued that these
236 haematite crystals are primary and precipitated when hot hydrothermal fluids (> 60 °C), rich
237 in reduced iron, mixed rapidly with seawater containing oxygen. Such a process for the
238 oxidation of dissolved ferrous (reduced) iron – entering the oceans from hydrothermal vents –
239 questions the common view of widespread anoxia throughout the early Archean (Konhauser,
240 2009). In our proposed deep subaqueous depositional model for the Marble Bar Chert
241 Member, these haematite particles may not be in situ sediments. Whatever their mechanism of
242 formation – i.e. transformation of a precursor lithology or direct precipitation from a silica-
243 rich fluid (cf. Van den Boorn *et al.* 2007) – dark-blue and red cherts were formed in
244 superficial environments and transported downslope by density currents. This challenges the
245 view of Hoashi *et al.* (2009) that Palaeoarchean deep (> 200 m) bottom ocean waters were at
246 least locally oxidizing.

247

248

249

250 **Acknowledgements.** This work was supported by a grant from CNRS-PID OPV and the
251 ChemCam program, Mars Science Laboratory project. N.F. acknowledges a Lavoisier grant
252 from the French Ministry of Foreign and European Affairs. PR, NF and NC acknowledge an
253 IPDF grant from the University of Sydney. The careful reviews of two anonymous reviewer
254 greatly improved this manuscript.

255
256
257
258
259
260
261
262
263
264
265
266
267
268
269
270
271
272
273
274
275
276
277
278

References

ALLWOOD, A. C., WALTER, M. R., KAMBER, B. S., MARSHALL, C. P. & BURCH, I. 2006. Stromatolite reef from the Early Archaean era of Australia. *Nature* **441**, 714–718.

BROUCKE, O., TEMPLE, F., ROUBY, D., ROBIN, C., CALASSOU, S., NALPAS, T. & GUILLOCHEAU, F. 2004. The role of deformation processes on the geometry of mud-dominated turbiditic systems, Oligocene and Lower–Middle Miocene of the Lower Congo basin (West African Margin). *Marine and Petroleum Geology* **21**, 321–348.

BUICK, R. & BARNS, K. R. 1984. Cherts in the Warrawoona Group: Early Archean silicified sediments deposited in shallow-water environments. *University of Western Australia, Geological Department & University Extension, Publication* **9**, 37–53.

BUICK, R., THORNETT, J.R., MCNAUGHTON, N.J., SMITH, J.B., BARLEY, M.E. & SAVAGE, M. 1995. Record of emergent continental crust 3.5 billion years ago in the Pilbara Craton of Australia. *Nature* **375**, 574–577.

DROMART, G., FERRY, S. & ATROPS, F. 1993. Allochthonous deep-water limestone conglomerates and relative sea-level changes: the Upper Jurassic-Berriasian of South-East France. In *Sequence stratigraphy and facies associations* (eds H. POSAMENTIER, C. SUMMERHAYES & G.P. ALLEN), pp. 295–305. International Association of Sedimentologists Special Publication 18.

FEDO, C. M., MYERS, J. S. & APPEL, P. W. U. 2001. Depositional setting and paleogeographic implications of earth's oldest supracrustal rocks, the 3.7 Ga Isua Greenstone belt, West Greenland. *Sedimentary Geology* **141-142**, 61–77.

279 GERVAIS, A., MULDER, N., SAVOYE, B., MIGEON, S. & CREMER, M.R. 2001. Recent processes
280 of levee formation on the Zaire deep-sea fan. *Comptes Rendus de l'Académie des Sciences*
281 *de Paris* **332**, 371–378.

282 HICKMAN, A. H. 1983. Geology of the Pilbara Block and its environs. *Western Australia*
283 *Geological Survey Bulletin* **127**, 1–268.

284 HICKMAN, A. H., & LIPPLE, S. L. 1978. Explanatory notes on the Marble Bar 1:250 000
285 Geological Sheet, Western Australia. *Geological Survey of Western Australia, Perth* 1–24.

286 HOASHI, M., BEVACQUA, D. C., OTAKE, T., WATANABE, Y., HICKMAN, A. H., UTSUNOMIYA,
287 S. & OHMOTO, H. 2009. Primary haematite in an oxygenated sea 3.46 billion years ago:
288 *Nature Geosciences* **2**, 301–306.

289 KATO, Y. & NAKAMURA, K. 2003. Origin and global tectonic significance of Early Archaean
290 cherts from the Marble Bar greenstone belt, Pilbara Craton, Western Australia.
291 *Precambrian Research* **125**, 191–243.

292 KOJIMA, S., HANAMURO, T., HAYASHI, K., HARUNA, M. & OHMOTO, H. 1998. Sulphide
293 minerals in Early Archaean chemical sedimentary rocks of the eastern Pilbara district,
294 Western Australia. *Mineralogy and Petrology* **64**, 219–235.

295 KONHAUSER, K. 2009. Deepening the early oxygen debate. *Nature Geosciences* **2**, 241–242.

296 LASCELLES, D. L. 2007. Black smokers and density currents: A uniformitarian model for the
297 genesis of banded iron-formations. *Ore Geology Reviews* **32**, 381–411.

298 MINAMI, M., SHIMIZU, H., MASUDA, A. & ADACHI, M. 1995. Two Archean Sm-Nd ages of
299 3.2 and 2.5 Ga for the Marble Bar Chert, Warrawoona Group, Pilbara Block, Western
300 Australia. *Geochemical Journal* **29**, 347–362.

301 MIGEON, S., SAVOYE, B., ZANELLA, E., MULDER, T., FAUGERES, J.-C. & WEBER O. 2001.
302 Detailed seismic-reflection and sedimentary study of turbidite sediment waves on the Var
303 Sedimentary Ridge (SE France): significance for sediment transport and deposition and for

304 the mechanisms of sediment-wave construction. *Marine and Petroleum Geology* **18**, 179–
305 208.

306 MUTTI, E. 1977. Distinctive thin-bedded turbidite facies and related depositional
307 environments in the Eocene Hecho Group (south-central Pyrenees, Spain). *Sedimentology*
308 **24**, 107–131.

309 MUTTI, E. & NORMARK, W. R. 1987. Comparing examples of modern and ancient turbidite
310 systems. In *Marine clastic sedimentology* (eds J. K. Legett & G. G. Zuffa), pp. 1–38.
311 Graham & Trotman [London].

312 NORMARK, W. R. & DAMUTH, J. E. 1997. Sedimentary facies and associated depositional
313 elements of the Amazon Fan. *Proceedings of the Ocean Drilling Program* **155**, 611–652.

314 NUTMAN, A. P. 2006. Antiquity of the oceans and continents. *Elements* **2**, 223–227.

315 OLIVER, N. S. H. & CAWOOD, P. A. 2001. Early Tectonic dewatering and brecciation on the
316 overturned sequence at Marble Bar, Pilbara Craton, Western Australia: dome-related or
317 not? *Precambrian Research* **105**, 1–15.

318 ORBERGER, B., ROUCHON, V., WESTALL, F., DE VRIES, S. T., PINTI, D. L., WAGNER, C.,
319 WIRTH, R. & HASHIZUME, K. 2006. Microfacies and origin of some Archean cherts
320 (Pilbara, Australia). In *Processes on the Early Earth* (eds W. U. Reimold & R. L. Gibson),
321 pp. 133–156, Geological Society of America Special Paper 405.

322 PIPER, D. J. W. & DEPTUCK, M. 1997. Fine-grained turbidites of the Amazon fan: facies
323 characterization and interpretation. *Proceedings of the Ocean Drilling Program* **155**, 79–
324 108.

325 PIPER, D. J. W. & STOW, D. A. V. 1991. Fine-grained turbidites. In *Cycles and Events in*
326 *Stratigraphy* (eds G. Einsele, W. Ricken & A. Seilacher), pp. 360–366. Springer-Verlag,
327 [New York].

- 328 RICHARDS, M., BOWMAN, M. & READING, H. 1998. Submarine-fan systems I:
329 characterization and stratigraphic prediction. *Marine and Petroleum Geology* **15**, 689–717.
- 330 ROBERT, F. & CHAUSSIDON, M. 2006. A palaeotemperature curve for the Precambrian oceans
331 based on silicon isotopes in cherts. *Nature* **443**, 969–972.
- 332 ROBIN, C. GORICAN, S. GUILLOCHEAU, F. RAZIN, P. DROMART, G. and MOSAFFA, H. 2010.
333 Mesozoic deep-water carbonate deposits from the southern Tethyan passive margin in Iran
334 (Pichakun nappes, Neyriz area): biostratigraphy, facies sedimentology and sequence
335 stratigraphy. In *Tectonic and Stratigraphic Evolution of Zagros and Makran during the*
336 *Mesozoic – Cenozoic* (eds P. LETURMY & C. ROBIN), pp. 179–210. Geological Society of
337 London, Special Publication 330.
- 338 ROSING, M. T. 1999. ¹³C-depleted carbon microparticles in > 3700-Ma sea-floor sedimentary
339 rocks from West Greenland. *Science* **283**, 674–676.
- 340 SCHOPF, J. W. 1993. Microfossils of the Early Archean Apex Chert: new evidence of the
341 antiquity of life. *Science* **260**, 640–646.
- 342 SCHOPF, J. W., KUDRYAVTSEV, A. B., AGRESTI, D. G., WDOWIAK, T. J. & CZAJA, A. D. 2002.
343 Laser-Raman imagery of Earth's earliest fossils. *Nature* **416**, 73–76.
- 344 SUGITANI, K. 1992. Geochemical characteristics of Archean cherts and other sedimentary
345 rocks in the Pilbara Block, Western Australia: evidence for Archean seawater enriched in
346 hydrothermally-derived iron and silica. *Precambrian Research* **57**, 21–47.
- 347 VAN DEN BOORN, S. H. J. M., VAN BERGEN, M. J., NIJMAN, W. & VROON, P. Z. 2007. Dual
348 role of seawater and hydrothermal fluids in Early Archean chert formation: Evidence from
349 silicon isotopes. *Geology* **35**, 939–942.
- 350 VAN DEN BOORN, S. H. J. M., VAN BERGEN, M. J., VROON, P. Z., DE VRIES, S. T. & NIJMAN,
351 W. 2010. Silicon isotope and trace element constraints on the origin of 3.5 Ga cherts:

352 Implications for Early Archaean marine environments. *Geochimica et Cosmochimica Acta*
353 **74**, 1077–1103.

354 VAN KRANENDONK, M. J. 2006. Volcanic degassing, hydrothermal circulation and the
355 flourishing of early life on Earth: A review of the evidence from c. 3490-3240 Ma rocks of
356 the Pilbara Supergroup, Pilbara Craton, Western Australia. *Earth Sciences Reviews* **74**,
357 197–240.

358 VAN KRANENDONK, M. J., SMITHIES, R. H., HICKMAN, A. H. & CHAMPION, D. C. 2007.
359 Review: secular tectonic evolution of Archean continental crust: interplay between
360 horizontal and vertical processes in the formation of the Pilbara Craton, Australia. *Terra*
361 *Nova* **19**, 1–38.

362

363

364 **FIGURE CAPTIONS**

365

366 Figure 1. Exposure of the Marble Bar Cherts at Chinaman and Marble Pools. (A) Geological
367 map of the Marble Bar area (simplified after Kato & Nakamura 2003). (B) Simplified
368 geological map of the Chinaman Pool area showing locations of measured sections.

369

370 Figure 2. The channel-levee depositional model for the Marble Bar Chert Member showing
371 illustration of the associated depositional facies. Orange dots are 5 cm across.

372

373 Figure 3. (A) Intra-formational breccia from the Chinaman Pool Section: monogenic, early-
374 lithified chert clasts inducing load casts during differential compaction (arrows). (B) Trough-
375 cross bedding in a coarse sand- to granule-size clastic deposit (upper section of the Marble
376 Bar Chert Member at Chinaman Pool).

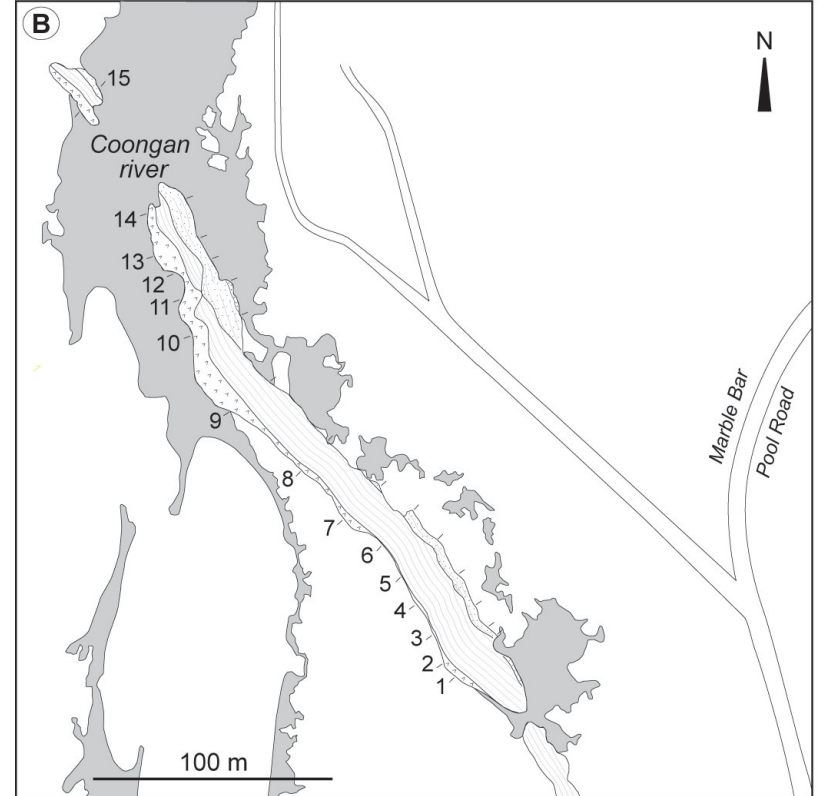
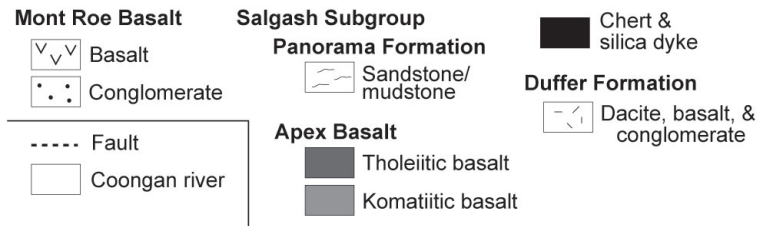
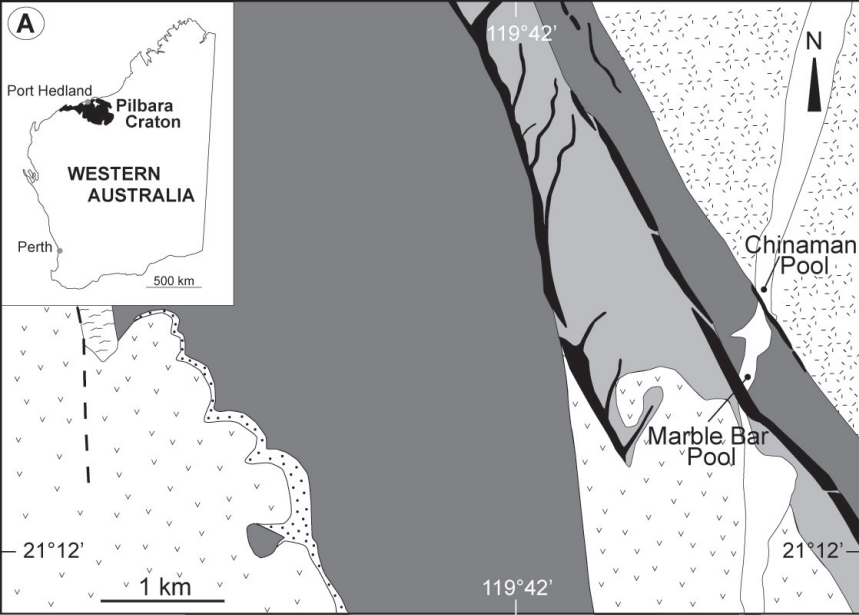


Figure 1 - Olivier *et al.*



Figure 3 - Olivier *et al.*